Wind Turbine Wake Characterizing using Coherent Wind Lidar

Songhua Wu, Xiaochun Zhai, Bingyi Liu, Changzhong Feng and Jintao Liu
Ocean Remote Sensing Institute, Ocean University of China
No. 238, Songling Road, Qingdao, China
wush@ouc.edu.cn

Abstract: Wind power is growing fast as one of the most promising renewable energy sources. When the wind turbine generator (WTG) extracts power from the wind, the wake evolves and leads to a considerable reduction in the efficiency of the actual power generation. The wake effect also leads to the increase of fatigue loads that reduce the life time of WTGs. In this work, a Pulsed Coherent Doppler Lidar (PCDL) is used to characterize the WTG wakes, which has high updating rate of 4 Hz and variable spatial resolution from 15 to 60 m. Field experiments were performed in the onshore and offshore wind parks from 2013 to 2015. Techniques based on a single Doppler Lidar were employed for elucidating main features of turbine wakes, including velocity deficit, wake dimension, velocity profile, 2D wind vector, turbulence dissipation rate and turbulence intensity under different conditions of surface roughness.

Keywords: Coherent Lidar, Wind turbine, Wake characteristics.

1. Introduction

Wind power generation is rapidly growing as one of the most promising renewable energy sources. When the turbine extracts power from the wind, the vortex evolves and moves downwind to form the turbine wake. Turbine wake characteristics of wind turbines have been studied since 1980s. Current industry standard for wind turbine wake measurements is the use of an in situ meteorological mast with wind cup and vane anemometers on it [1]. Because of the global growth of wind energy, techniques such as ultrasonic anemometer, profilers and SODAR (Sonic Detection and Ranging) are increasingly being used to measure wind wake [2].

As compared with the techniques mentioned above, the coherent Doppler Lidar (Light Detection and Ranging) has enabled high spatial and temporal resolution measurements of wind fields [3]. Krishnamurthy et al. presented the utilization of a commercial WindTracer Lidar to calculate spatially varying wind power density distribution in an ongoing wind assessment study [4]. The research of wind turbine wake detected by a continuous-wave CDL was done by Bingöl et al. [5] and Trujillo et al. [6]. Jungo et al [7] used scanning Lidar to analyze the velocity components over the vertical symmetry plane of the wind turbine wake. Banta et al. [8] studied the 3D structure of turbine wake using 3D volume scan patterns by a 2 μm wavelength high peak power laser system, which was a part of a field campaign generally reported by Smalikho et al. [9].

The objective of this paper is to use a PCDL with relatively high spatial resolution and sampling rate to visualize the WTGs wakes and to characterize the geometry and dynamics of wakes. The PCDL specifications and retrieval methods are described in Section 2. Field experiments to visualize and characterize WTG wakes are described in Section 3. A brief conclusion is given in Section 4.

2. Methodology

The PCDL is based on all-fiber laser technology and fast digital-signal-processing technology [10]. Because of the all-fiber structure adoption, the system is stable, reliable and high-integrated. In order to capture turbine wakes, different scan strategies are used to scan horizontal or vertical sections back and forth to track the wake. The highlights of the Lidar include the flexible range resolution from 15 to 60 m and

relatively high sampling rate. The finest resolution of 15 m is useful for the detection of small scale wakes. The duration of measurement of one LOS velocity equals 0.25 s, which increases the temporal sampling rate up to 4 Hz and therefore reduces uncertainty in an averaged wind measurement.

The initial velocity deficit depends on the amount of momentum extracted by the turbine from the ambient flow, and the velocity deficit in a wake is defined as:

$$VD(z) = \frac{\bar{v}_{amb}(z) - v_{wake}(z)}{\bar{v}_{amb}(z)} \times 100\% \quad (1)$$

where $\bar{v}_{amb}(z)$ is the mean ambient wind velocity outside of the wake, and $v_{wake}(z)$ is the minimum velocity at each range gate distance z within the wake downstream, quantifying the downwind extent of the wake. The wake length is defined to be the location where the $VD(z)$ has minimum value. Figure 2 (a) shows that the location of these minimum values, plotted as black plus signs, were not necessarily located symmetrically within the wake, and the ambient wind velocity is shown in blue solid line. Figure 2 (b) shows the velocity deficit behind WTG A, and it can be seen that the maximum velocity deficit and wake length is 44.95 %, 0.63 km, respectively.

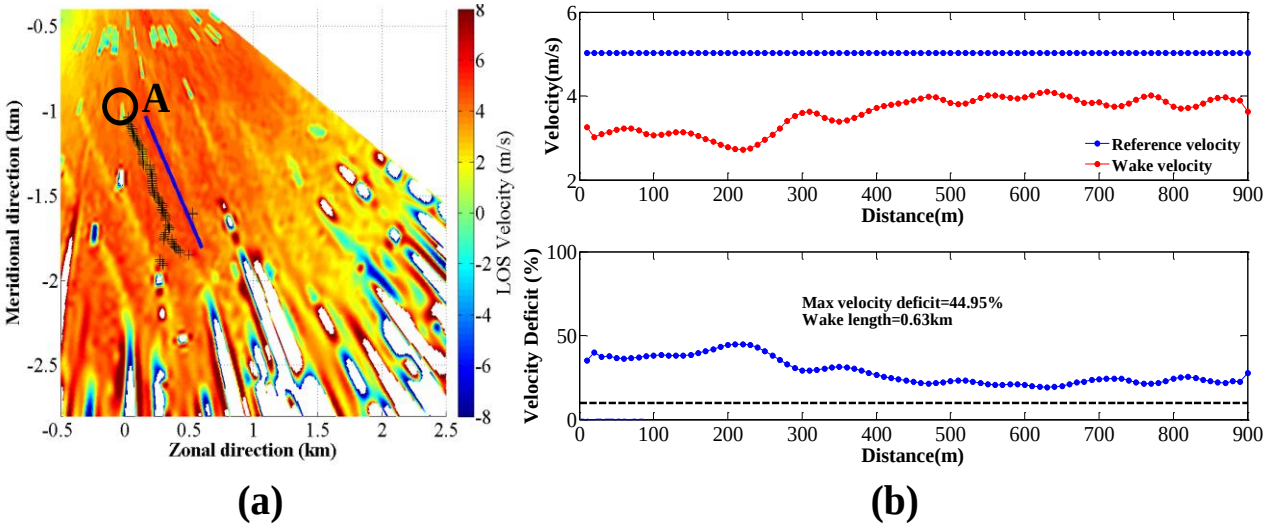

Figure 2. (a) Conical sector scan performed at an elevation angle of 1.5° at 1930 BJT 15 Nov, 2014 in Hami gobi desert wind park, (b) Ambient wind velocity in red dot, wake area velocity in blue dot (upper), and the corresponding velocity deficit in blue dot (bottom)

To analyze the influence of atmospheric turbulence on the turbine wake using PCDL, the 2D wind field by arc PPI measurements is used. The turbulence energy dissipation rate (TEDR) is retrieved based on the structure function of 2D LOS wind velocity. Herein the transverse structure function is used to retrieve the TEDR since it has better vertical resolution and the errors, introduced by the anisotropy, is smaller than the longitudinal structure function's. This method has been described in detail by Frehlich and Cornman [11]. Figure 3 shows the structure function using different models. From the fit to the $D_{wgt-calculate}(s)$, we derived the value of $\sigma = 0.540 \ \ m/s$ and $L_0 = 147.4 \ \ m$, then the values for $L_i = 110.1 \ \ m$ and $\varepsilon = 0.001 \ \ m^2/s^3$ can be calculated from Equation.2, Equation.3, respectively.

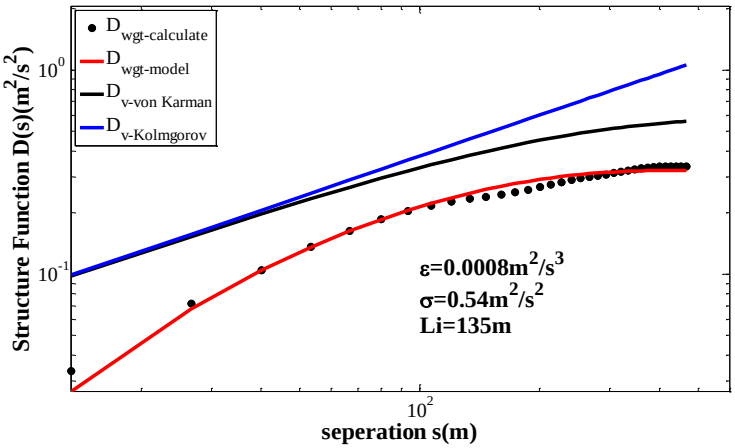

Figure 2. Transverse structure function estimates of turbulence using single PPI scanning at 1833 BJT 10 April, 2014 in Rudong tidal zone wind park with an elevation angle $\theta = 3^{\circ}$ range-gate distance $R = 1.275km$.

$$\varepsilon = [\frac{2^{1/3}\pi}{\sqrt{3}\Gamma(1/3)\Gamma(4/3)}]\frac{\sigma^3}{L_0} = 0.933668\frac{\sigma^3}{L_0} \tag{2}$$

$$L_i = \frac{\sqrt{\pi}\Gamma(5/6)}{\Gamma(1/3)}L_0 = 0.7468343L_0 \tag{3}$$

3. Results

In order to understand the wake characteristics in a real ambient, we performed field experiments with different topographies and surface roughness to study the turbulent wind field in the vicinity of operating WTGs in the onshore and offshore wind parks from 2013 to 2015. The first field campaign was carried out in Longgang mountain wind park shown in Figure 3 (a). The complex terrain can cause inhomogeneous flow conditions and disturb turbine wakes with more complicated behaviors. The second and third field campaign were carried out in Rudong tidal zone wind park shown in Figure 3 (b). The water covered surface and mud flat in the intertidal zone produced a more homogeneous surface with lower roughness, hence producing distinct turbine wakes with extended its longitudinal dimensions as shown in Figure 4 (b). The fourth field experiment was performed at Hami gobi desert wind park with a flat desert topography shown in Figure 3 (c). In the Lidar measurements at Gobi plain area, turbines formed wide and long wakes extending for 2 km as shown in Figure 4 (c).

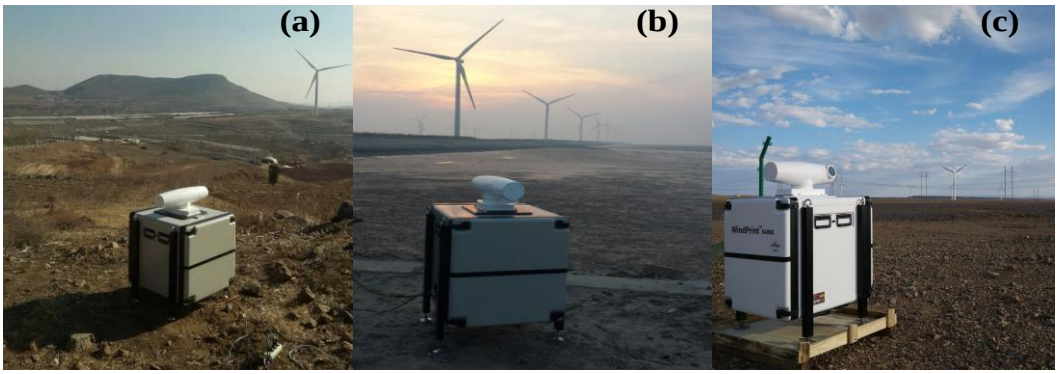

Figure 3. Wind flow measurement with PCDL in (a) Longgang Mountain (b) Rudong tidal zone and (c) Hami gobi desert area.

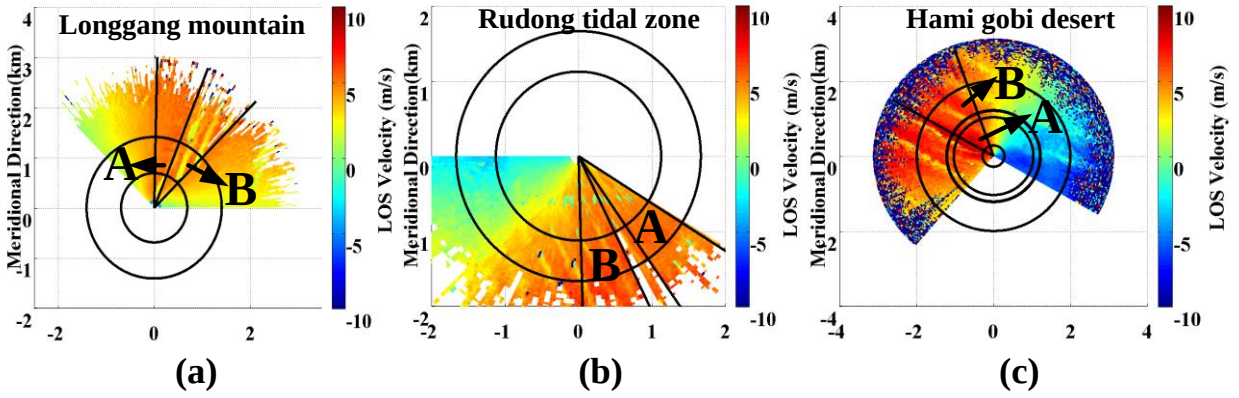

Figure 4. LOS wind field by PCDL PPI scanning mode at (a) Longgang Mountain, (b) Rudong tidal zone (c) Hami gobi desert area. The area A and B is the chosen ambient wind field and wake area, respectively.

In order to quantitatively compare the turbulent characteristics in the wind turbine wake area and ambient wind field in different topographies, the area with relatively distinct wake structures should be chosen as the wake area, which is marked A in Figure 4. Conversely, the ambient wind field which is seldom affected by the wind turbine is chosen marked B in Figure 4. After the determination of ambient wind area and corresponding wake area, the turbulent parameters including the TEDR ε, LOS turbulence intensity I_{LOS}, the standard deviation of transverse velocity fluctuations σ_{LOS}, turbulence integral scale L_i can be retrieved using structure function method mentioned above.

Figure 5 shows the averaged turbulence characteristics in ambient wind area A and wake area B in three wind parks, respectively. It can be seen that the experiment was mostly carried out under conditions of weak turbulence ($10^{-3} \le \varepsilon \le 10^{-2}$), and Rudong tidal zone ambient wind area has relatively higher I_{LOS} and σ_{LOS}, since during the measurements, the sea surface temperature was 14°C - 15.4 °C along the coastline and higher than the air temperature around 13°C in the nighttime. This temperature gradient may bring in surface turbulence created by thermal convection. As for the wake area, Longgang mountain area and Rudong tidal zone area have transferred into strong turbulence condition, however, although the ε in Hami gobi desert wake area is more than 10 times of its ambient wind areas', it is still in relative weak turbulence conditions. Different surface roughness may lead to obviously different turbulence characteristics in these areas.

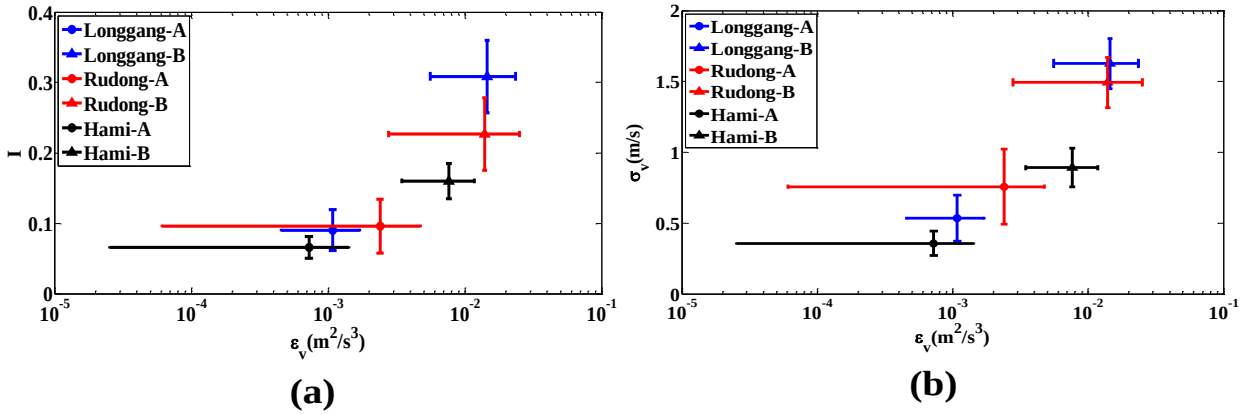

Figure 5. Averaged turbulence characteristics in ambient wind area and wake area under three wind parks

4. Conclusion

In this research, four field experiments with different topographies and surface roughness have been carried out to study the turbulent wind field in the vicinity of operating WTGs in the onshore and offshore wind parks. The turbulence characteristics such as the turbulence energy dissipation rate and turbulence intensity have been retrieved and compared quantitatively in ambient wind area and wake area under different topographies in the analyzed time period. It is found that the ε , I_{LOS} and σ_{LOS} in wake area is 7.8, 2.6, 2.3 times of the ambient areas', respectively. All of these three ambient areas are in the weak turbulence conditions. On the contrary, Longgang mountain area and Rudong tidal zone area have transferred into strong turbulence condition in wake areas, but it is still in relative weak turbulence conditions in Hami gobi desert wake area, showing different surface roughness may lead to obviously different turbulence characteristics in these areas.

Acknowledgements

This work was partly supported by the National Natural Science Foundation of China (NSFC) under grant 41471309 and 41375016.

5. References

[1] F. B. Amar, M. Elamouri, and R. Dhifaoui, "Energy assessment of the first wind farm section of Sidi Daoud, Tunisia," Renew. Energy A **33**(10), 2311–2321 (2008).
[2] R. J. Barthelmie, G. C. Larsen, S. T. Frandsen, L. Folkerts, K. Rados, S. C. Pryor, B. Lange, and G. Schepers, "Comparison of wake model simulations with offshore wind turbine wake profiles measured by sodar," J. Atmos. Oceanic Technol. A **23**(7), 888–901 (2006).
[3] U. Högström, D. N. Asimakopoulos, H. Kambezidis, C. G. Helmis, and A. Smedman, "A field study of the wake behind a 2MW wind turbine," Atmos. Environ. A **22**(4), 803–820 (1988).
[4] R. Krishnamurthy, A. Choukulkar, R. Calhoun, J. Fine, A. Oliver, and K. Barr, "Coherent Doppler lidar for wind farm characterization," Wind Energy (Chichester Engl.) **16**(2), 189–206 (2013).
[5] F. Bingöl, J. Mann, and G. C. Larsen, "Light detection and ranging measurements of wake dynamics, part I: onedimensional scanning," Wind Energy A **13**(1), 51–61 (2010).
[6] J. Trujillo, F. Bingol, G. Larsen, J. Mann, and M. Kuhn, "Light detection and ranging measurements of wake dynamics. Part II: Two-dimensional scanning," Wind Energy A **14**(1), 61–75 (2011).
[7] G. Iungo, Y. Wu, and F. Porteagel, "Field Measurements of Wind Turbine Wakes with Lidars," J. Atmos. Ocean. Technol. **30**(2), 274–287 (2013).
[8] G. Iungo, Y. Wu, and F. Porteagel, "Field Measurements of Wind Turbine Wakes with Lidars," J. Atmos. Ocean. Technol. **30**(2), 274–287 (2013).
[9] I. N. Smalikho, V. A. Banakh, Y. L. Pichugina, W. A. Brewer, R. M. Banta, J. K. Lundquist, and N. D. Kelley, "Lidar investigation of atmosphere effect on a wind turbine wake," J. Atmos. Oceanic Technol. A **30**(11), 2554–2570 (2013).
[10] S. H. Wu, B. Y. Liu, J. T. Liu, X. C. Zhai, C. Z. Feng, G. N. Wang, H. W. Zhang, J. P. Yin, X. T. Wang, R. Z. Li, D. Gallacher, "Wind turbine wake visualization and characteristics analysis by Doppler lidar," Opt Express, **24**(10), A762-A780 (2016).
[11] R. Frehlich and L. Cornman, "Estimating spatial velocity statistics with coherent Doppler lidar," J. Atmos. Ocean. Technol. **19**(3), 355–366 (2002).